Electronic Supplementary Material (ESI) for Physical Chemistry Chemical Physics.

SUPPORTING INFORMATION

Procedure to determine the separation distance between electrodes:

A customized assembly with a (6.9 ± 0.1) µm thick transparent TiO_2 mesoporous layer was sealed either with Surlyn polymer or with epoxy resin and the separation between electrodes was determined with a micrometer for both configurations. The results show a separation of (21.9 ± 1.9) µm and (7.4 ± 1.0) µm for the Surlyn and epoxy configurations, respectively. These measurements show that the separation between FTO glass electrodes in the so called "epoxy cells" is basically the thickness of the mesoporous transparent layer. The difference between the separation of electrodes of the epoxy cells and the average value of thickness of the mesoporous layer can be attributed to the thicker edges usually present in screen printed samples, which determines the ultimate separation in epoxy cells. The separation between the last layer of mesoporous TiO_2 in the working electrode and the PEDOT counter electrode in cells sealed with Surlyn polymer will be around 16 – 17 µm whereas for the epoxy cells, there will be virtually no separation.

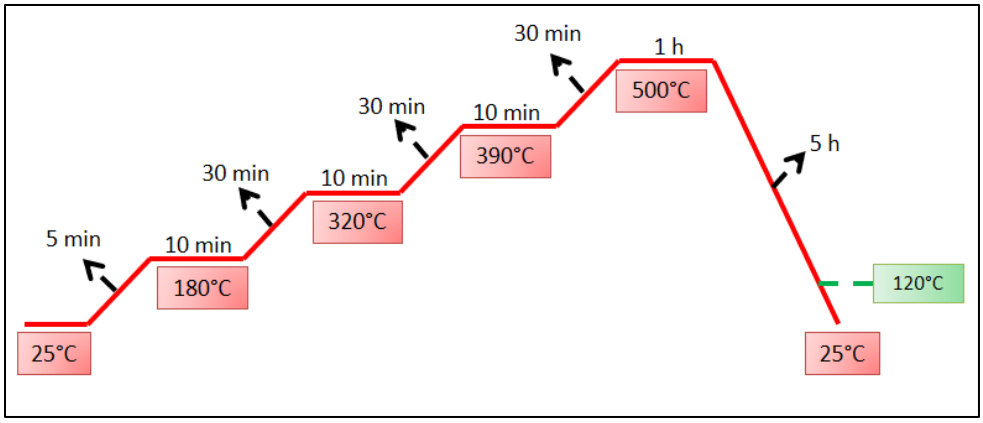

Figure S1. Sintering temperature ramp for the 0.25 cm^2 working electrodes. When films are heat-treated prior to dye loading, the process is halted at 120 °C.

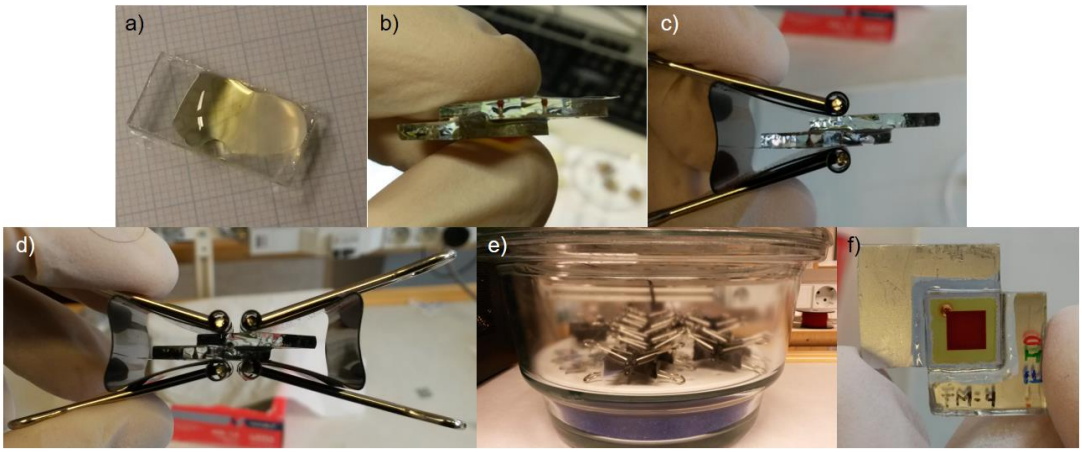

Figure S2. (**a**) Mixture 1:1 Solaronix Amosil 4R [Bisphenol-A-(epichlorhydrin) epoxy resin] and 4H (2,2'-iminodiethylamine). (**b**) Electrode and counter electrode pressed against each other. (**c**) Using paper clamps to keep together the electrodes, the epoxy glue is applied on the edges where the two electrodes meet. (**d**) and (**e**) Once the epoxy glue is applied, the cell is kept under the pressure of two paper clamps and they are put inside a desiccator in the dark and the epoxy resin cures overnight. (**f**) The cells are filled with the electrolytic solution and sealed.

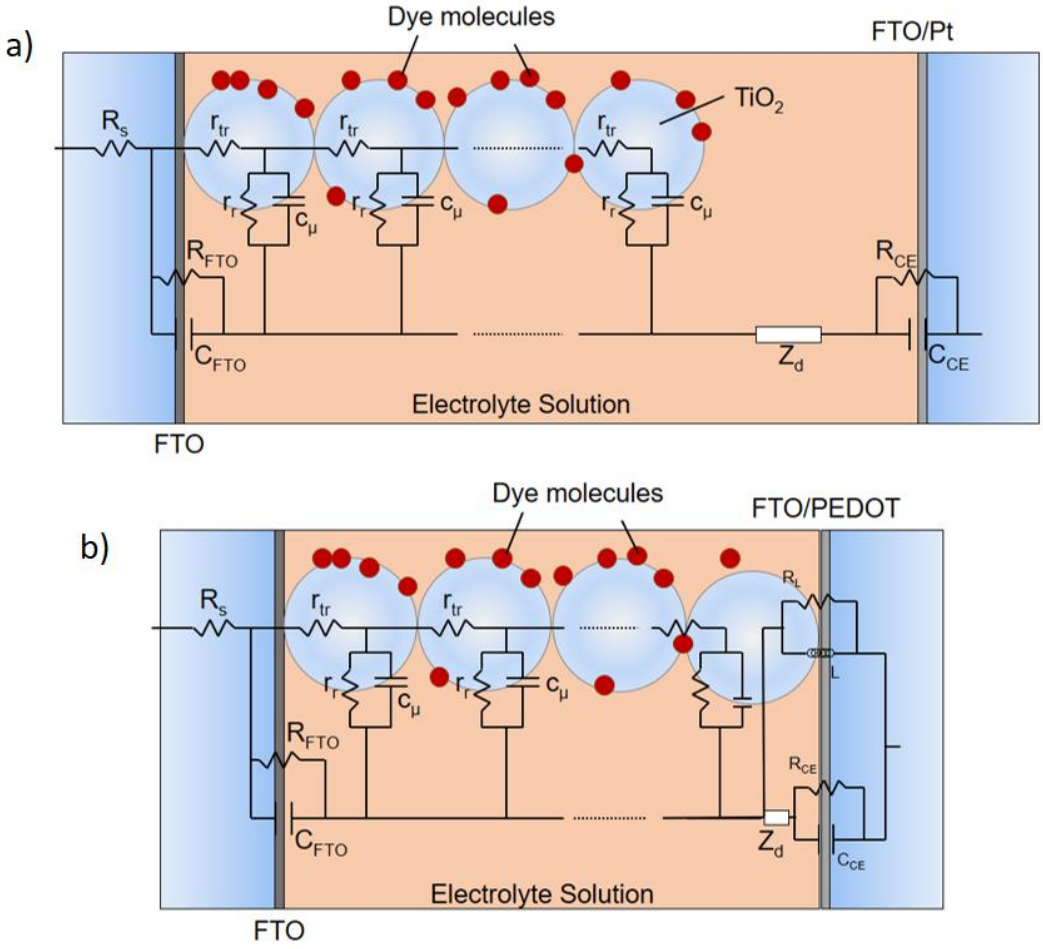

Figure S3. General equivalent circuit model used to fit impedance spectroscopy results for (**a**) Surlyn cells and Epoxy-ZrO_2 cells and (**b**) Epoxy-TiO_2 cells.

In Figure S3, R_s represents the series resistance of the FTO; R_{FTO} and C_{FTO} stand for the elements of resistance and capacitance for the recombination via the substrate uncovered by the TiO_2 nanoparticles; r_{tr} represents the resistance for electron transport along the metal oxide nanoparticles; r_r is the charge transfer resistance that exists to the process of recombination between electrons in the metal oxide and the redox species in the electrolytic solution; c_μ is the chemical capacitance; Z_d is the Warburg impedance of the diffusion of the redox species in the electrolytic solution; R_{CE} stands for the charge transfer resistance that exist at the counter electrode/electrolyte interface and C_{CE} represents the Helmholtz capacitance at the counter electrode/electrolyte interface[1]. R_L and L represent the interaction between electrons in the TiO_2 and the PEDOT counter electrode.

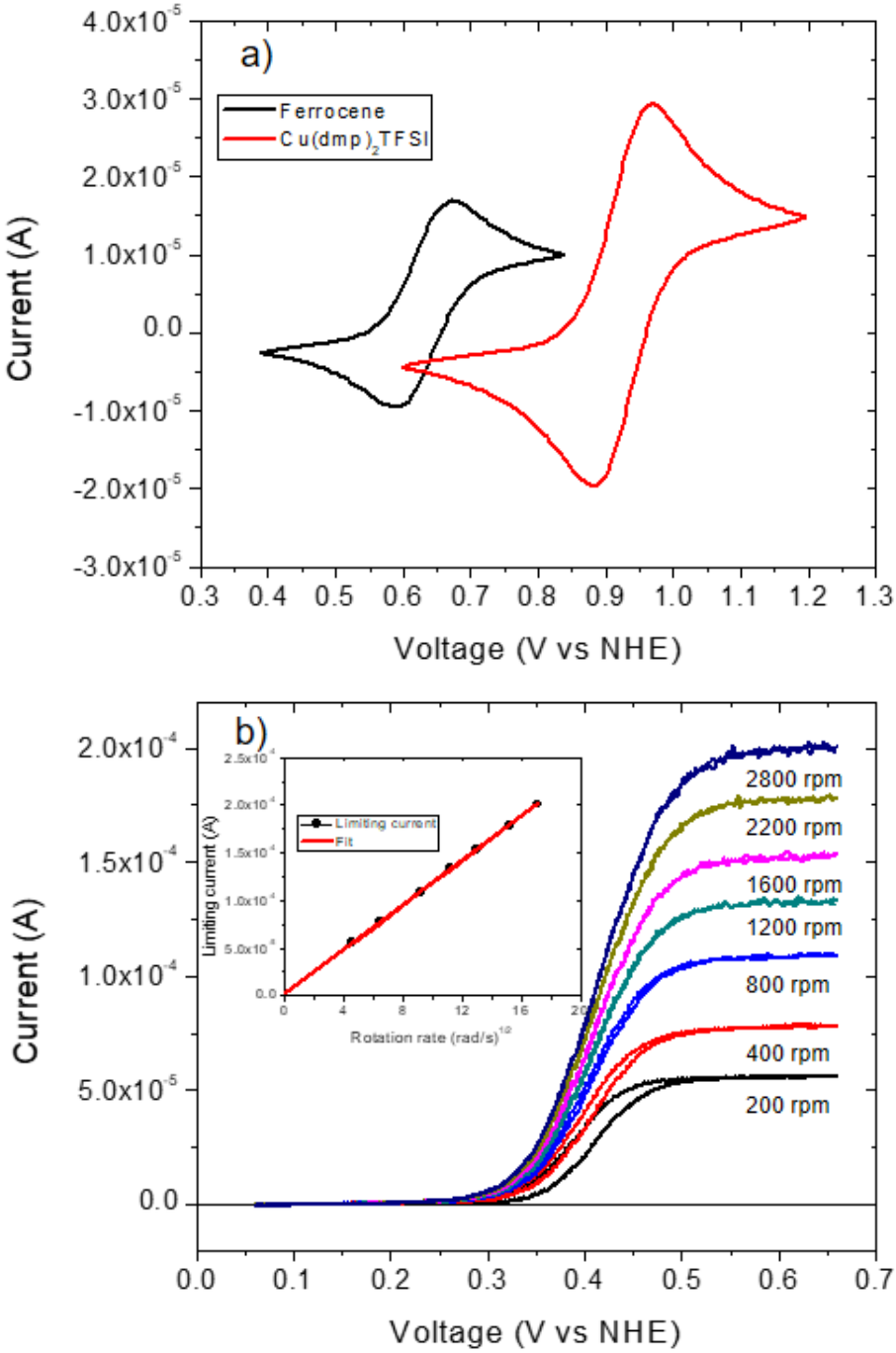

Figure S4. (**a**) Cyclic voltammogram of 5 mM $Cu(dmp)_2TFSI$ in 0.1 M $TBAPF_6$ solution in acetonitrile. The cyclic voltammogram for Fc/Fc^+ (0.63 vs NHE) was used to calibrate the reference electrode potential before the experiments and is also presented in the figure. In (b) the RDE measurements at different angular velocities are plotted. The inset in (**b**) shows the linear dependence of the limiting current and the angular velocity.

In Figure S4 (**b**) the diffusion coefficient was calculated using the Levich equation[2]:

$$i_{l,c} = 0.62nFAD_0{}^{2/3}\omega^{1/2}\nu^{-1/6}C_0^* \quad \text{(S1)}$$

where $i_{l,c}$ is the limiting current in Amperes, n is the number of electrons involved in the redox reaction, A is the area of the working electrode in cm^2, D_0 is the diffusion coefficient of the redox specie in cm^2/s, ω is the angular velocity of the working electrode in rad/s, ν is the kinematic viscosity in cm^2/s and C_0* is the bulk concentration of the redox specie in mol/cm^3. The area of the working electrode was 3.1 x 10^{-2} cm^2.

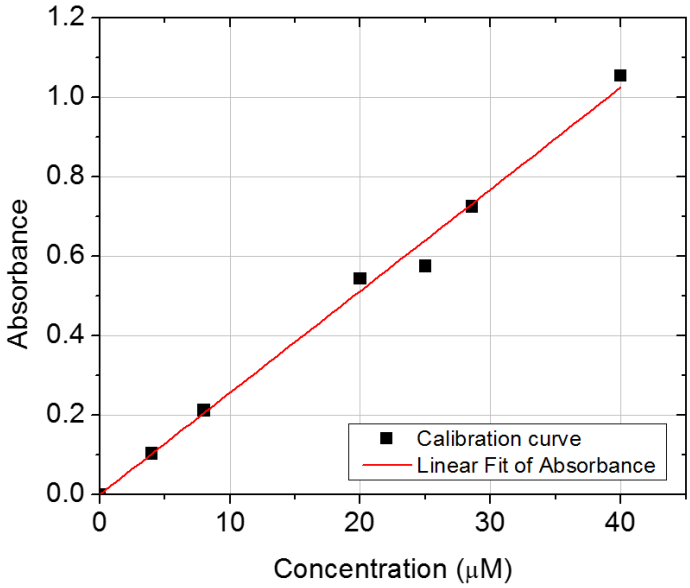

Figure S5. Calibration curve in dye desorption measurements. The values of absorbance were obtained at a wavelength of 480.75 nm.

Table S1. Concentration of dye adsorbed in the mesoporous electrodes obtained with dye desorption measurements.

Electrode	*Concentration in the film (mol/cm^2)*
5.3 μm TiO_2	(8.3 ± 0.9) x 10^{-8}
5.3 μm TiO_2 + 0.4 μm ZrO_2	(9.4 ± 0.9) x 10^{-8}

When a reverse bias is applied in the cell, the following electrochemical reaction should take place at the FTO in the working electrode:

$$[Cu(dmp)_2]^+ \rightarrow [Cu(dmp)_2]^{2+} + 1e^- \quad \text{(S2)}$$

If the voltage is large enough a maximum value of current is obtained. This saturation current density, J_{lim}, is related to the transport of the ionic carriers from one electrode to the other[3–5], and its value will depend on diffusion limitations of the oxidized specie ($[Cu(dmp)_2]^{2+}$), since its concentration is lower than the reduced specie ($[Cu(dmp)_2]^+$). The reverse bias measurements applied to the three different configurations are presented in Figure S6 (**a**) and reverse bias measurements for the epoxy-TiO_2 cells with different thickness of the mesoporous layer is displayed in Figure S6 (**b**).

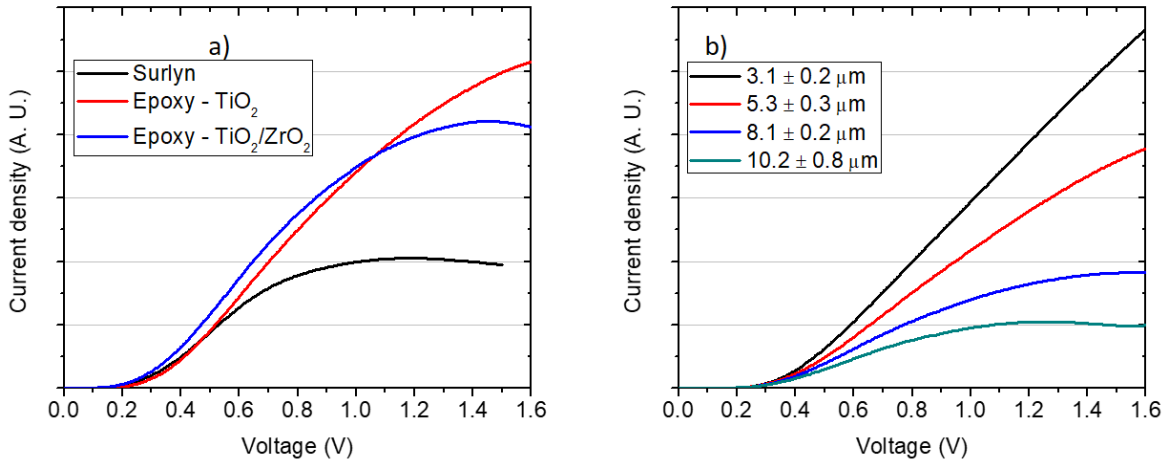

Figure S6. (**a**) Reverse bias measurements for the different cell configurations. (**b**) Reverse bias measurements for the epoxy–TiO_2 cells with different mesoporous layer thicknesses.

Figure S6 (**b**) shows the effect of the mesoporous layer thickness on the limiting current attainable under reverse bias. This figure show how as the thickness of the mesoporous layer is increased, the limiting current decreases, due to the increase of the distance that the redox couple must diffuse to react, reducing the concentration gradient of the redox couple inside the cell and thus, reducing the flux of ions towards the working electrode. A remarkable difference between cell configurations can also be observed in Figure S6 (**a**). Here, the limiting current value obtained for Surlyn cells is lower than the value obtained for the epoxy-TiO_2/ZrO_2 cells, highlighting the influence of the distance between electrodes. This imply that the diffusion of the $Cu(dmp)_2$ redox couple in the bulk may be an important factor limiting the attainable current in the device, when usually the diffusion of the redox couple in the mesoporous layer is the only factor considered. When comparing epoxy-TiO_2 and epoxy- TiO_2/ZrO_2 cells, the limiting current for the latter seems to be somewhat lower, while no limiting current value seems to be reached for the former, even at potentials as high as 1.6 V. This difference between both epoxy configurations may be due to the extra ZrO_2 mesoporous layer, which increases the thickness of the mesoporous layer which may decrease the concentration gradient of the redox couple inside the DSC, altering the flux of charge inside the cell.

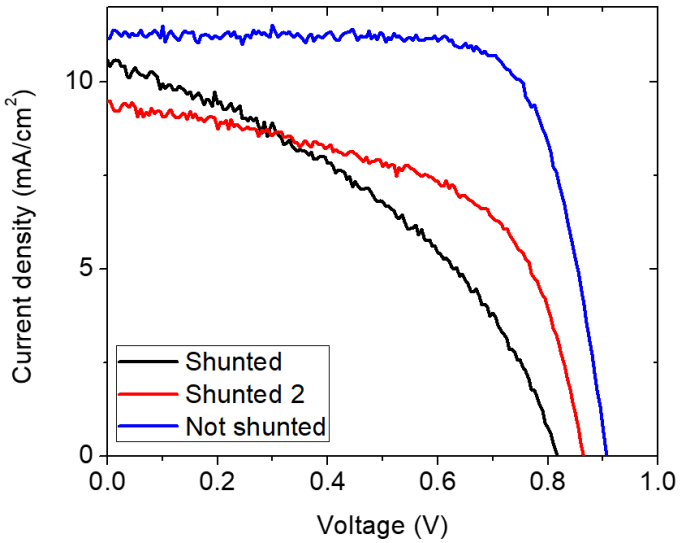

Figure S7. Representation of shunted and non-shunted epoxy-TiO_2 cells.

Determination of the electronic lifetime

The product between charge transfer recombination and chemical capacitance gives the electronic lifetime:

$$\tau_n = R_{ct} C_\mu \quad \text{(S3)}$$

The electronic lifetime is the time an electron will prevail in the mesoporous layer before it recombines. It is a central quantity to determine recombination dynamics in the DSC[6].

REFERENCES

1 F. Fabregat-Santiago, G. Garcia-Belmonte, I. Mora-Seró and J. Bisquert, *Phys. Chem. Chem. Phys.*, 2011, **13**, 9083–9118.

2 A. J. Bard and L. R. Faulkner, *Electrochemical methods. Fundamentals and Applications.*, John Wiley & Sons, Inc., Second Edi., 2001.

3 F. Fabregat-Santiago, J. Bisquert, E. Palomares, L. Otero, D. Kuang, S. M. Zakeeruddin and M. Grätzel, *J. Phys. Chem.*, 2007, **2**, 6550–6560.

4 E. Guillén, C. Fernández-Lorenzo, R. Alcántara, J. Martín-Calleja and J. A. Anta, *Sol. Energy Mater. Sol. Cells*, 2009, **93**, 1846–1852.

5 J. M. Vicent-Luna, J. Idígoras, S. Hamad, S. Calero and J. A. Anta, *J. Phys. Chem. C*, 2014, **118**, 28448–28455.

6 J. Bisquert, A. Zaban, M. Greenshtein and I. Mora-Seró, *J. Am. Chem. Soc.*, 2004, **126**, 13550–13559.